The Finite-Difference Time-Domain Solution of Lossy MTL Networks with Nonlinear Junctions

Doru Mardare and Joe LoVetri, *Member, IEEE*

Abstract— **In this paper, we describe a numerical technique to solve lossy multiconductor transmission line (MTL) networks, also known as tube/junction networks, which contain nonlinear lumped circuits in the junctions. The method is based on using a finite-difference technique to solve the time-domain MTL equations on the tubes, as well as the modified nodal analysis (MNA) formulation of the nonlinear lumped circuits in the junctions. The important consideration is the interface between the MTL and MNA regimes. This interface is accomplished via the first and last finite-difference current/voltage pair on each MTL of the network and, except for this, the two regimes are solved independently of each other. The advantage of the FDTD method is that the MTL equations may contain distributed source terms representing the coupling with an external field. We apply the method to previously published examples of multiconductor networks solved by other numerical methods, and the results agree exceptionally well. The case of an externally coupled field is also considered.**

I. Introduction

In a general electromagnetic topology we encounter all three of the classical electromagnetic regimes: lumped circuit, distributed parameter, and field problems. All three regimes can be formulated as time-domain differential equations, with the main difference being the number of space dimensions. Multiconductor transmission line (MTL) networks, i.e., tubes and junctions [1], are ubiquitously present in electromagnetic topology problems, where one is interested in the flow of electromagnetic energy from one part of the topology to another. Thus, the solution of these networks from an electromagnetic compatibility, as well as functional standpoint, is important. The representation of the junctions as black-boxes characterized by measured or calculated S-parameters is an important technique which can give a useful approximation of the energy levels flowing in the topology [2]. These methods are based on the BLT equation approach, which is a frequency-domain analysis [1] for which various methods of approximation have been published [2], [3]. Simultaneously, many numerical solution techniques have been published by groups interested in the operational aspects of MTL networks [4]–[8]. From an EMC standpoint, where the coupling of an external field to the MTL is of interest, the finite-difference time-domain method has been used previously for a single MTL [9], [10], but not for tube/junction networks. The ability to solve these networks with nonlinear junctions and external field coupling is an important aspect of the finite-difference time-domain procedure described herein.

Manuscript received June 20, 1994; revised December 1, 1994.

The authors are with the Department of Electrical Engineering, University of Western Ontario, London, ON N6A 5B9 Canada.

IEEE Log Number 9410256.

Thus, as an initial step to solving a complete electromagnetic topology problem, we describe the time-domain solution of general MTL networks with nonlinear lumped circuit junctions. It is important that we accomplish the interface between the lumped and distributed regimes at the numerical level, using an interface condition which couples the two time-domain solutions and not by incorporating the lumped model equations into the MTL equations, or vice versa. The reason is that strict adherence to this paradigm will make it simpler to interface a time-domain field modeler to the code in the future.

II. Time-Domain MTL Network Formulation

The time-domain formulation of multiconductor transmission line problems (in the TEM approximation) has been known for a long time (see, for example, [12], [13]). The MTL's, or tubes, can be described by a system of partial differential equations in (x,t), and so explicit finite-difference equations can be obtained and solved, subject to boundary and initial conditions [14]. The voltage and current on an $n+1$ conductor MTL are described by the coupled partial differential equations

$$\frac{\partial}{\partial x}\boldsymbol{V}(x,t) + \boldsymbol{L}\frac{\partial}{\partial t}\boldsymbol{I}(x,t) + \boldsymbol{R}\boldsymbol{I} = \boldsymbol{V}^s(x,t) \quad (1)$$

$$\frac{\partial}{\partial x}\boldsymbol{I}(x,t) + \boldsymbol{C}\frac{\partial}{\partial t}\boldsymbol{V}(x,t) + \boldsymbol{G}\boldsymbol{V} = \boldsymbol{I}^s(x,t) \quad (2)$$

where $\boldsymbol{V}(x,t)$ [V] and $\boldsymbol{I}(x,t)$ [A] are column vectors of the n voltages and currents on the MTL, and $\boldsymbol{V}^s(x,t)$ [V/m] and $\boldsymbol{I}^s(x,t)$ [A/m] are the column vectors of the n distributed voltage and current sources produced by, for instance, an external electromagnetic field. The $n \times n$ matrices $\boldsymbol{L}, \boldsymbol{R}, \boldsymbol{C}$, and $\boldsymbol{G}$ are the per unit inductance, resistance, capacitance, and conductance matrices describing the MTL. If these matrices are constant with respect to x, then the MTL is said to be uniform. In the more general case, these are a function of frequency to take into account the dispersive nature of the MTL (due to such phenomena as the skin effect).

Many of these MTL tubes can be connected in a tube-junction topology, as shown in Fig. 1, where the junctions represent a connection of the MTL's through some sort of lumped network [1], [4]. The objective is to calculate the current or voltage at any point in the topology, given the sources in the lumped network (i.e., junctions) and/or distributed sources on the tubes. We do this by using a finite difference technique in the time-domain, as will be described.

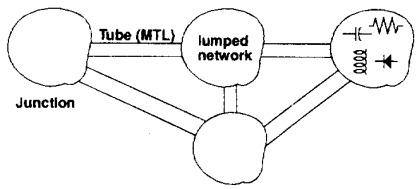

Fig. 1. Tube-junction topology.

III. Numerical Solution of Tube-Junction Topology

Time-domain methods have been suggested in the past for this problem. In [4], several techniques are presented to calculate the time-domain response of multiconductor transmission lines. A time stepping solution is based on discretizing the transmission line equations in space and time, and it is shown to be the same as solving a lumped-circuit equivalent of the transmission line by the Euler method. Unfortunately, the forward-time, center-space, time stepping scheme chosen by Djordjevic *et al.* is unstable, and a time-step one twentieth that suggested by the Courant limit, was required. This biased the CPU resource requirements for their code to seem greater than is actually necessary—for example, when a center-time, center-space, time stepping scheme, such as in [10], is used.

Djordjevic *et al.* also describe a time-domain modal analysis technique, which can only be applied to lossless lines with frequency-independent parameters [4]. It can be easily interfaced to the analysis of terminal networks, which may contain nonlinear elements. Modal analysis in the frequency-domain can be applied to lossy lines, which may have frequency-dependent parameters. The terminal networks must contain only linear elements in this case. The fast Fourier transform (FFT) is used to obtain the time-domain response.

The last technique described in [4] is based on the evaluation of the line Green's functions (i.e., the line responses to delta-function excitation). This method can be applied to the most general case of lossy transmission lines with nonlinear terminal networks. No reference is made in [4] to the coupling with an external incident EM field, or to the response of MTL networks.

In [10], the time-domain transmission line equations for uniform transmission lines excited by a transient nonuniform EM field are derived from Maxwell's equations. The transmission line equations are then discretized by a time-space centered finite-difference technique. The analysis is limited to a single multiconductor transmission line section, terminated at both ends. In [11], time-domain modal analysis is applied to lossless tube networks. The scattering matrix for the junction is used to calculate the transmitted and reflected waves at the junction. The scattering matrix is calculated using KCL and KVL at the lossless junction. The method assumes that there are no lumped elements in the junction—just branches (tubes) interconnected to one another.

In [7], a method is developed for analyzing the time-domain response of systems consisting of an arbitrary number of multiconductor transmission lines, which can be mutually interconnected and terminated by linear networks. The frequency-domain response is found and, by applying the inverse FFT, the time-domain response can be evaluated. This approach has difficulty when the analysis must span a time interval of several line transient time, because of the large number of points that must be added to the analysis to avoid aliasing problems. In [8], an alternative approach based on the numerical inversion of the Laplace transform is presented. The formulation is based on the modified nodal analysis (MNA) [16] for describing the transmission lines, the terminal, and the interconnecting networks. The method was not applied to the case of MTL coupling with an external EM field.

Recently, Tang and Nakhla [6] have proposed a new method for the transient analysis of lossy transmission line coupled networks, including nonlinear elements. The method combines the asymptotic waveform evaluation technique with a piecewise decomposition algorithm. The equations describing the transmission line system and the equations describing the terminal and interconnecting networks are formulated using the modified nodal analysis. The approach in [6] doesn't treat the external coupling case.

The method we chose to discretize the MTL equations is an explicit time-space centered finite-difference scheme, similar to that described by Agrawal *et al.* in [10]. The final update equations are written in matrix form as

$$\boldsymbol{I}_{k+1/2}^{n+1/2}=\left(\frac{\boldsymbol{L}}{\Delta t}+\frac{\boldsymbol{R}}{2}\right)^{-1}\left[\frac{I_{k+1/2}^{S^{n-1/2}}}{2}\left(\frac{\boldsymbol{L}}{\Delta t}-\frac{\boldsymbol{R}}{2}\right)\boldsymbol{I}_{k+1/2}^{n-1/2}-\frac{\boldsymbol{V}_{k+1}^{n}-\boldsymbol{V}_{k}^{n}}{\Delta x}+\frac{\boldsymbol{V}_{k+1/2}^{S^{n+1/2}}+\boldsymbol{V}_{k+1/2}^{S^{n-1/2}}}{2}\right] \tag{3}$$

with $k = 1, 2, \cdots, km - 1$, and

$$\boldsymbol{V}_{k}^{n+1}=\left(\frac{\boldsymbol{C}}{\Delta t}+\frac{\boldsymbol{G}}{2}\right)^{-1}\left[\frac{I_{k+1/2}^{S^{n-1/2}}}{2}\left(\frac{\boldsymbol{C}}{\Delta t}-\frac{\boldsymbol{G}}{2}\right)\boldsymbol{V}_{k}^{n}-\frac{\boldsymbol{I}_{k+1/2}^{n+1/2}-\boldsymbol{I}_{k-1/2}^{n+1/2}}{\Delta x}+\frac{\boldsymbol{I}_{k}^{S^{n+1}}+\boldsymbol{I}_{k}^{S^{n}}}{2}\right] \tag{4}$$

with k =1, 2, $\cdots$, km where $km = D/\Delta x$, and D is the line length. This is equivalent to approximating each MTL as a series of T-cells. A three-line ($n = 2$) MTL example is shown in Fig. 2.

We specify the lumped circuits at the junctions, using the modified nodal analysis (MNA) technique, described in [15], [16], and couple the MTL equations to the MNA equations via the last half-section of T-cells at each junction. It is important to use a coupling scheme which preserves the stability of the update equations (which will be described next).

IV. Formulation and Solution of the Junction Network Equations

On each MTL, the finite-difference scheme used is space and time centered and, in the spirit of the Yee algorithm, the voltage and current variables are interlaced in space and

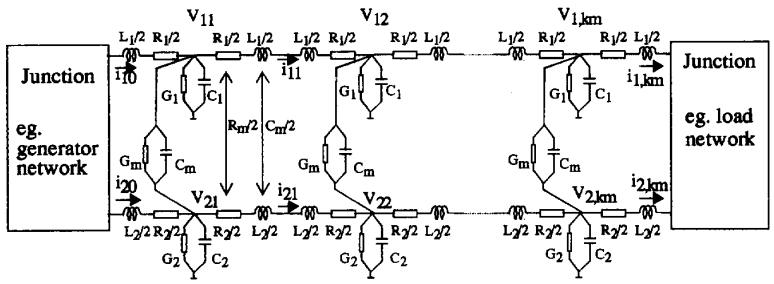

Fig. 2. T-cell discretization of MTL with $n = 2$ (no distributed sources).

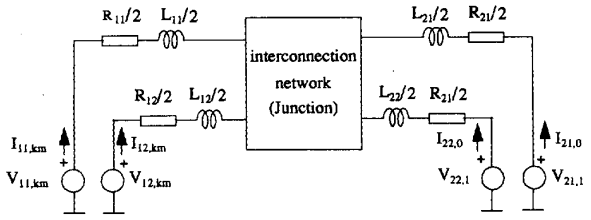

Fig. 3. Interconnection model between two MTL's.

time. In [9] and [10], the terminal currents are obtained by extrapolating the currents at the closest two current nodes. The form of the extrapolation may pose stability problems for the FDTD scheme [17], especially in the case of MTL networks. We chose to introduce these terminal currents as unknowns in the lumped model of the terminal and interconnecting networks.

We specify the lumped circuits, using the modified nodal analysis (MNA) technique, described in [15], [16], and couple the MTL equations to the MNA equations, via the last half-section of T-cells at each junction. Fig. 3 shows the model for the interconnection of two MTL's each with $n = 2$. $V_{11,km}$ and $V_{12,km}$ represent the voltages on the last voltage node of the first MTL. $V_{21,1}$ and $V_{22,1}$ are the voltages on the first voltage node of the second MTL. $R_{11}, R_{12}, L_{11}, L_{12}$ and $R_{21}, R_{22}, L_{21}, L_{22}$ are the per-unit-length parameters (resistance and inductance) of the first and second MTL, respectively. At each time step, the lumped network is solved and the currents at the terminal ends of the lines ($I_{11,km}, I_{12km}, I_{21,0}$ and $I_{22,0}$) are determined, so that the voltages at all the voltage nodes along the MTL's can be calculated using the FDTD updating scheme.

In the general case of a linear network, the s-domain network equations can be expressed as

$$\underline{\boldsymbol{Y}}(s)\underline{\boldsymbol{X}}(s) = \underline{\boldsymbol{W}}(s) \tag{5}$$

where $\underline{\boldsymbol{Y}}(s)$ represents the modified nodal admittance matrix, $\underline{\boldsymbol{X}}(s)$ is the unknown vector which includes the nodal voltages and the branch currents introduced by the additional constitutive relations for the branches that contains voltage sources or current controlled elements. The source vector $\underline{\boldsymbol{W}}(s)$ includes the values of voltage and current sources, as well as initial conditions for capacitors or inductors.

In the time-domain, the elements of the modified nodal matrix $\boldsymbol{Y}$ can be stored in two constant matrices: a matrix $\boldsymbol{D}$ that includes the values of $\boldsymbol{Y}$ which are not coefficients of partial derivative terms in the network equations; and a matrix $\boldsymbol{E}$ that includes the values of $\boldsymbol{Y}$ which are coefficients of partial derivatives (i.e., coefficients containing the Laplace variable, s) in the network equations. Thus, in the time-domain (5) becomes

$$\boldsymbol{DX} + \boldsymbol{EX}' = \boldsymbol{W} \quad \text{or} \quad \boldsymbol{EX}' = \boldsymbol{W} - \boldsymbol{DX}. \tag{6}$$

The matrices $\boldsymbol{D}$ and $\boldsymbol{E}$ are determined in a straightforward manner by using stamps for ideal lumped elements [15], [16].

If we consider the backward Euler formula with time-step Δt

$$\boldsymbol{X}'(n+1) = \frac{1}{\Delta t}(\boldsymbol{X}^{n+1} - \boldsymbol{X}^n) \tag{7}$$

then the finite difference formula for (6) becomes

$$\boldsymbol{EX}^{n+1} = \boldsymbol{EX}^n + \Delta t(\boldsymbol{W}^{n+1} - \boldsymbol{DX}^{n+1}) \tag{8}$$

$$\left(\boldsymbol{D} + \frac{1}{\Delta t}\boldsymbol{E}\right)\boldsymbol{X}^{n+1} = \frac{1}{\Delta t}\boldsymbol{EX}^n + \boldsymbol{W}^{n+1} \tag{9}$$

and the explicit update equation can be written as

$$\boldsymbol{X}^{n+1} = \boldsymbol{M1} \cdot \boldsymbol{X}^n + \boldsymbol{M2} \cdot \boldsymbol{W}^{n+1} \tag{10}$$

where

$$\boldsymbol{M1} = \left(\boldsymbol{D} + \frac{1}{\Delta t}\boldsymbol{E}\right)^{-1}\frac{1}{\Delta t}\boldsymbol{E},$$

$$\boldsymbol{M2} = \left(\boldsymbol{D} + \frac{1}{\Delta t}\boldsymbol{E}\right)^{-1}. \tag{11}$$

As can be seen from Fig. 3, the source term W for a terminal or interconnecting network contains, in addition to the independent sources present in the network, equivalent voltage sources representing the terminal voltage nodes on the individual lines in the MTL. The variables (i.e., unknowns) in X in which we are interested, are the terminal currents on the lines since these are required in the MTL update equations. In Fig. 3, these are $I_{11,km}, I_{12,km}, I_{21,0}$, and $I_{22,0}$. If the time-step at which we determine these currents is $n+1/2$, then the equivalent voltage sources in W corresponding to the terminal voltage nodes on the lines will be those calculated at time n. In the updating relation (10), the only term that needs to be updated at every time-step is the source vector W. The matrix inversion is computed just once, at the beginning of the computation.

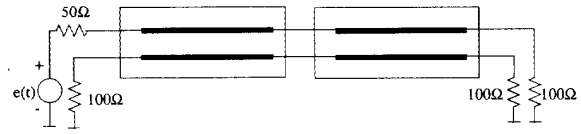

Fig. 4. Direct interconnection of two MTL's.

A. Validation of the Interface Condition

To validate the use of the MNA formulation for junctions interconnecting two MTL's, we consider two identical lossless MTL's, as shown in Fig. 4. Each MTL is a 3 conductor line (i.e., $n = 2$) 1.4 [m] in length and is characterized by the per-unit-length inductance and capacitance matrices

$$L = \begin{bmatrix} 494.6 & 63.3 \\ 63.3 & 494.6 \end{bmatrix} [\text{nH/m}]$$

$$C = \begin{bmatrix} 60.054 & -7.685 \\ -7.685 & 60.054 \end{bmatrix} [\text{pF/m}].$$

The equivalent lumped circuit of the direct interconnection between the MTL's is shown in Fig. 5, where $L_1 = L_{11}\Delta x$, $L_2 = L_{22}\Delta_z$ and $L_m = (\Delta z/2)[L_{12}+L_{21}]$, L_m being the total mutual inductance between the two lines.

The MTL's are assumed to be embedded in a homogeneous medium, so they have equal mode velocities: $v_1 = v_2 = 1.85 \times 10^8$ [m/s]. The MNA matrices required in (10), (11) are:

$$D = \begin{bmatrix} 0 & 0 & 0 & 0 & 1 & 1 & 0 & 0 & 0 & 0 \\ 0 & 0 & 0 & 0 & 0 & -1 & 1 & 0 & 0 & 0 \\ 0 & 0 & 0 & 0 & 0 & 0 & 0 & 1 & 1 & 0 \\ 0 & 0 & 0 & 0 & 0 & 0 & 0 & 0 & 0 & 1 \\ 1 & 0 & 0 & 0 & 0 & 0 & 0 & 0 & 0 & 0 \\ 1 & -1 & 0 & 0 & 0 & 0 & 0 & 0 & 0 & 0 \\ 0 & 1 & 0 & 0 & 0 & 0 & 0 & 0 & 0 & 0 \\ 0 & 0 & 1 & 0 & 0 & 0 & 0 & 0 & 0 & 0 \\ 0 & 0 & 1 & -1 & 0 & 0 & 0 & 0 & 0 & 0 \\ 0 & 0 & 0 & 1 & 0 & 0 & 0 & 0 & 0 & 0 \end{bmatrix}$$

$$E = \begin{bmatrix} 0 & 0 & 0 & 0 & 0 & 0 & 0 & 0 & 0 & 0 \\ 0 & 0 & 0 & 0 & 0 & 0 & 0 & 0 & 0 & 0 \\ 0 & 0 & 0 & 0 & 0 & 0 & 0 & 0 & 0 & 0 \\ 0 & 0 & 0 & 0 & 0 & 0 & 0 & 0 & 0 & 0 \\ 0 & 0 & 0 & 0 & 0 & 0 & 0 & 0 & 0 & 0 \\ 0 & 0 & 0 & 0 & 0 & -L_1 & 0 & 0 & -L_m & 0 \\ 0 & 0 & 0 & 0 & 0 & 0 & 0 & 0 & 0 & 0 \\ 0 & 0 & 0 & 0 & 0 & 0 & 0 & 0 & 0 & 0 \\ 0 & 0 & 0 & 0 & 0 & -L_m & 0 & 0 & -L_2 & 0 \\ 0 & 0 &) & 0 & 0 & 0 & 0 & 0 & 0 & 0 \end{bmatrix}$$

$$\boldsymbol{X} = [V_{n1} \quad V_{n2} \quad V_{n3} \quad V_{n4} \quad I_{11,km}^{n+1/2} \quad I_{L_1} \quad I_{21,0}^{n+1/2} \quad I_{12,km}^{n+1/2} \quad I_{L_2} \quad I_{22,0}^{n+1/2}]^T$$

$$\boldsymbol{W} = [0 \quad 0 \quad 0 \quad 0 \quad V_{11,km}^{n} \quad 0 \quad V_{21,1}^{n} \quad V_{12,km}^{n} 0 \quad V_{22,1}^{n}]^T.$$

The voltage source $e(t)$ is a 1 [V] rectangular pulse with a rise/fall time of 1.5 [ns] and a total duration of 5.5 [ns]. The voltage waveforms along the driven lines of the two MTL's are shown in Fig. 6, at different time-steps. The time-step size was calculated using the Courant stability condition: $\Delta t = \Delta x/v$, and our space step was set to $\Delta x = 1$ [cm]. As can be seen from the figure, the square pulse propagates across the junction without any numerical reflection. This result gives us confidence that the method will perform well when more complicated junctions are introduced.

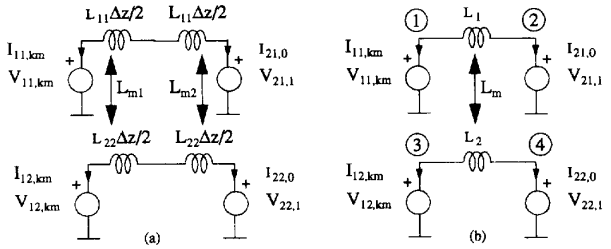

Fig. 5. Interconnecting lumped model for circuit in Fig. 4: (a) initial; (b) simplified.

V. Terminal and Interconnecting Networks with Nonlinear Elements

In the case of nonlinear lumped networks, there is no change in the topological equations since the KVL and KCL equations are independent of the branch relations. The description of a nonlinear element is given in implicit form. That is, for nonlinear resistive, capacitive, and inductive branches, the implicit equation can be expressed as

$$p(v_R, i_R) = w_R, \quad C(v_C, q_C) = 0, \quad \text{and} \quad L(i_L, \phi_L) = 0 \tag{12}$$

respectively, where q_C and ϕ_L are the capacitor charge and inductor flux. The constitutive equations for branches with nonlinear capacitors and inductors are given by the linear differential relations $i_C = q_C'$ and $v_L = \phi_L'$, respectively.

To incorporate the nonlinear elements in the modified nodal formulation, the capacitor charges and inductor fluxes are introduced as variables in the vector of unknowns $\boldsymbol{X}$ [15]. This will increase the size of the system, but the differential equations become linear and the nonlinearities are transformed into algebraic equations. Thus, the modified nodal formulation can be written in the form

$$\boldsymbol{f}(\boldsymbol{X}', \boldsymbol{X}, \boldsymbol{W}, t) \equiv \boldsymbol{E}\boldsymbol{X}' + \boldsymbol{D}\boldsymbol{X} + \boldsymbol{p}(\boldsymbol{X}) - \boldsymbol{W} = \boldsymbol{0} \tag{13}$$

where $\boldsymbol{D}$ and $\boldsymbol{E}$ are, as before, constant matrices which describe the linear lumped elements and independent sources. The nonlinear components in the network are collected in the term $\boldsymbol{p}(\boldsymbol{X})$, $\boldsymbol{X}$ represents the vector of unknowns, and $\boldsymbol{W}$ is the source vector.

The nonlinear analysis problem reduces now to one of solving the set of algebraic-differential equations (13). In choosing the solution method, of particular importance is the stability and convergence properties of the algorithm used. The solution method we chose is based on using a first order backward differentiation formula to approximate the derivative in, and the Newton–Raphson iteration technique for solving the derived corrector equation [15], [18].

We obtain accurate results by using the first order predictor formula, given by

$$\boldsymbol{X}_{n+1}^{P} = 2\boldsymbol{X}_n - \boldsymbol{X}_{n-1} \tag{14}$$

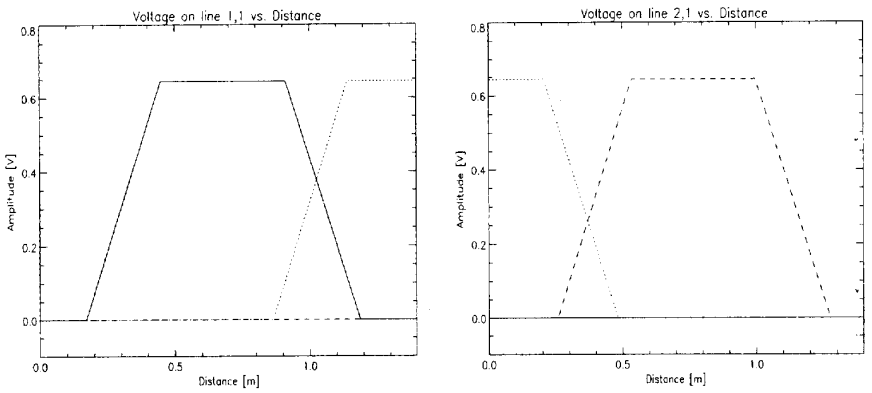

Fig. 6. Voltages on the driven lines. The p.u.l parameter matrices L and C satisfy the TEM condition: $LC = I/v_p^2$. Time step: (——) 120; (· · ·) 190; (- - -) 270.

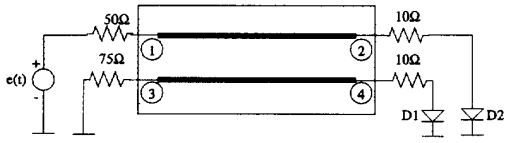

Fig. 7. Single MTL ($n = 2$) with nonlinear loads.

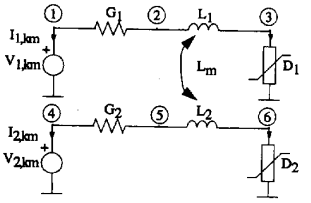

Fig. 8. Equivalent circuit of the nonlinear terminal network for the MNA formulation.

and corrector formula given by

$$(\boldsymbol{X}')^i_{n+1} = \frac{1}{\Delta t}(\boldsymbol{X}^i_{n+1} - \boldsymbol{X}_n), \quad \boldsymbol{X}^0_{n+1} = \boldsymbol{X}^P_{n+1} \tag{15}$$

which is the well-known backward Euler formula. Note that here we are now using subscripts n to denote the time-step and superscripts i to denote the iteration number. The vector $\boldsymbol{X}'_{n+1}$ found via this scheme is used in the discretized version of (13) given as

$$\begin{aligned}\boldsymbol{f}^i_{n+1}&((\boldsymbol{X}')^i_{n+1}, \boldsymbol{X}^i_{n+1}, \boldsymbol{W}^i_{n+1}, t)\\ &= \boldsymbol{E}(\boldsymbol{X}')^i_{n+1} + \boldsymbol{D}\boldsymbol{X}^i_{n+1} + \boldsymbol{p}(\boldsymbol{X}^i_{n+1}) - \boldsymbol{W}^i_{n+1} \approx \boldsymbol{0}\end{aligned} \tag{16}$$

which is then solved for $\boldsymbol{X}^i_{n+1}$ using the Newton–Raphson algorithm. That is, at each time-step the Newton–Raphson iteration proceeds as follows

$$\boldsymbol{M}^i_{n+1}\Delta\boldsymbol{X}^i_{n+1} = -\boldsymbol{f}^i_{n+1} \tag{17}$$

$$\begin{aligned}\boldsymbol{X}^{i+1}_{n+1} &= \boldsymbol{X}^i_{n+1} + \Delta\boldsymbol{X}^i_{n+1}\\ \boldsymbol{X}^0_{n+1} &= \boldsymbol{X}^P_{n+1}\end{aligned} \tag{18}$$

where $\boldsymbol{M}^i_{n+1}$ is the Jacobian matrix and can be written as

$$\boldsymbol{M}_{n+1} = \left(\frac{1}{\Delta t}\right)\boldsymbol{E} + \boldsymbol{D} + \frac{\partial \boldsymbol{p}}{\partial \boldsymbol{X}_{n+1}}. \tag{19}$$

The iterations proceeds until the error norm is less than a predefined value $||\Delta\boldsymbol{X}^i_{n+1}|| \leq \varepsilon$.

To avoid the long operation of matrix inversion of the Jacobian at each iteration, (17) can be solved for $\Delta\boldsymbol{X}^i_{n+1}$ by LU factorization. Sparse matrix methods can also be used because the nonzero elements of the Jacobian matrix are fixed by the circuit topology and remain unchanged from iteration to iteration. The Newton–Raphson algorithm has a fast quadratic convergence when started close to the solution, and since our time-step is limited by the time-step of the MTL algorithm, there is no need for a more accurate solution method.

In summary, the algorithm we use to solve the nonlinear terminal or interconnecting lumped networks can be specified as follows [15].

1) Predict $\boldsymbol{X}^P_{n+1}$ using the predictor formula (14).
2) Calculate $\boldsymbol{X}'_{n+1}$ using (15).
3) Calculate the vector function $\boldsymbol{f}^i_{n+1}$, (16).
4) Calculate the Jacobian (19).
5) Apply the Newton–Raphson iteration (17) and (18).
6) If the error norm condition is not satisfied, go back to Step 2.

Stamps for nonlinear elements, similar to those used for linear networks, can be used to fill in the entries in the Jacobian [15].

A. Nonlinear Termination Example

We now apply this method to an MTL with nonlinear termination. Consider the coupled three-conductor (i.e., $n = 2$) lossy transmission line shown in Fig. 7. This configuration was solved by Djordjevic *et al.* using a Green's function method [19]. We use a line length of 0.5 [m], and the transmission line parameter matrices are given as

$$\boldsymbol{L} = \begin{bmatrix} 309 & 21.7 \\ 21.7 & 309 \end{bmatrix} \text{[nH/m]}$$

$$\boldsymbol{C} = \begin{bmatrix} 144 & -6.4 \\ -6.4 & 144 \end{bmatrix} \text{[pF/m]}$$

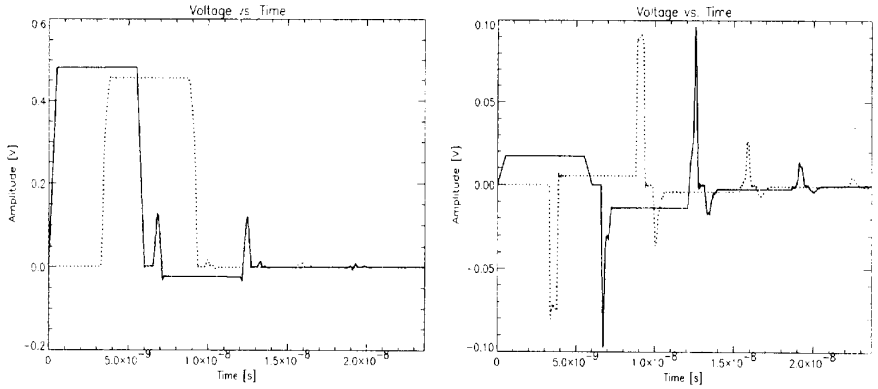

Fig. 9. Terminal voltages of single MTL shown in Fig. 7. Left: (——) node 1, (- - -) node 2; Right: (——) node 3, (- - -) node 4.

$$\boldsymbol{R} = \begin{bmatrix} 524 & 33.9 \\ 33.9 & 524 \end{bmatrix} [\mathrm{m}\Omega/\mathrm{m}]$$

$$\boldsymbol{G} = \begin{bmatrix} 905 & -11.8 \\ -11.8 & 905 \end{bmatrix} [\mathrm{nS/m}].$$

In [19], the resistances and the conductances were assumed to vary with frequency. Currently we neglect this variation, but have found almost no difference with the results given in [19]. The active line is driven by a 1 [V] rectangular voltage source with an internal resistance of 50 [Ω], a rise and fall time of 0.5 [ns], and a total duration of 6 [ns]. At the right-hand side the lines are terminated in a series combination of a 10 [Ω] resistor and a diode. The characteristic of the diode is given by

$$i_D = I_A\left(\exp\left(\frac{v}{V_T}\right) - 1\right) \tag{20}$$

with $I_A = 10$ [nA] and $V_T = 25$ [mV].

The equivalent circuit of the nonlinear load termination for the MNA formulation is shown in Fig. 8. The circuit elements in the figure are given by

$$G_1 = \frac{1}{R_{11}(\Delta x/2) + 10}\,[\mathrm{S}], \quad G_2 = \frac{1}{R_{22}(\Delta x/2) + 10}\,[\mathrm{S}],$$

$$L_1 = L_2 = L_{11}(\Delta x/2)\,[\mathrm{H}], \quad L_m = L_{12}(\Delta x/2)\,[\mathrm{H}],$$

and the matrices necessary to determine $\boldsymbol{f}_{n+1}$ of (16) are as shown at the bottom of this page, and

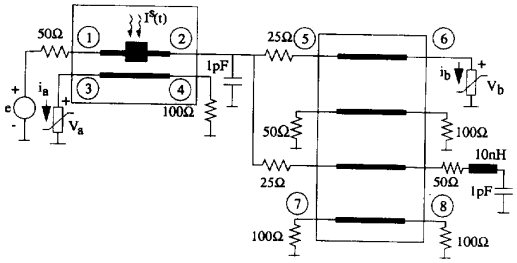

Fig. 10. Tang and Nakhla interconnect model with lossy MTL's.

$$\boldsymbol{X} = [V_{n1} \quad V_{n2} \quad V_{n3} \quad V_{n4} \quad V_{n5} \quad V_{n6} \quad I_{1,km} \quad I_{L1} \quad I_{2,km} \quad I_{L2}]^T$$

$$\boldsymbol{p} = \left[0 \quad 0 \quad I_A\left(\exp\left(\frac{V_{n3}}{V_T}\right) - 1\right) \quad 0 \quad 0 \quad I_A\left(\exp\left(\frac{V_{n6}}{V_T}\right) - 1\right) \quad 0 \quad 0 \quad 0 \quad 0\right]^T$$

$$\boldsymbol{W} = [0 \quad 0 \quad 0 \quad 0 \quad 0 \quad 0 \quad V_{1,km} \quad 0 \quad V_{2,km} \quad 0]^T$$

where V_{n1} to V_{n6} are the voltages at nodes 1–6, shown in Fig. 8.

The line is discretized using a spatial step size of $\Delta x = 2$ [mm]. The mode velocities (calculated from the eigenvalues of the product matrix $\boldsymbol{LC}$, with a lossless conductors assumption) are $v_1 = 1.52127 \times 10^8$ [m/s] and $v_2 = 1.482428 \times 10^8$

$$\boldsymbol{D} = \begin{bmatrix} G1 & -G1 & 0 & 0 & 0 & 0 & 1 & 0 & 0 & 0 \\ -G1 & G1 & 0 & 0 & 0 & 0 & 0 & 1 & 0 & 0 \\ 0 & 0 & 0 & 0 & 0 & 0 & 0 & -1 & 0 & 0 \\ 0 & 0 & 0 & G2 & -G2 & 0 & 0 & 0 & 1 & 0 \\ 0 & 0 & 0 & -G2 & G2 & 0 & 0 & 0 & 0 & 1 \\ 0 & 0 & 0 & 0 & 0 & 0 & 0 & 0 & 0 & 1 \\ 1 & 0 & 0 & 0 & 0 & 0 & 0 & 0 & 0 & 0 \\ 0 & 1 & -1 & 0 & 0 & 0 & 0 & 0 & 0 & 0 \\ 0 & 0 & 0 & 0 & 1 & 0 & 0 & 0 & 0 & 0 \\ 0 & 0 & 0 & 0 & 1 & -1 & 0 & 0 & 0 & 0 \end{bmatrix} \quad \boldsymbol{E} = \begin{bmatrix} 0 & 0 & 0 & 0 & 0 & 0 & 0 & 0 & 0 & 0 \\ 0 & 0 & 0 & 0 & 0 & 0 & 0 & 0 & 0 & 0 \\ 0 & 0 & 0 & 0 & 0 & 0 & 0 & 0 & 0 & 0 \\ 0 & 0 & 0 & 0 & 0 & 0 & 0 & 0 & 0 & 0 \\ 0 & 0 & 0 & 0 & 0 & 0 & 0 & 0 & 0 & 0 \\ 0 & 0 & 0 & 0 & 0 & 0 & 0 & 0 & 0 & 0 \\ 0 & 0 & 0 & 0 & 0 & 0 & 0 & 0 & 0 & 0 \\ 0 & 0 & 0 & 0 & 0 & 0 & 0 & -L_1 & 0 & -L_m \\ 0 & 0 & 0 & 0 & 0 & 0 & 0 & 0 & 0 & 0 \\ 0 & 0 & 0 & 0 & 0 & 0 & 0 & -L_m & 0 & -L_2 \end{bmatrix}$$

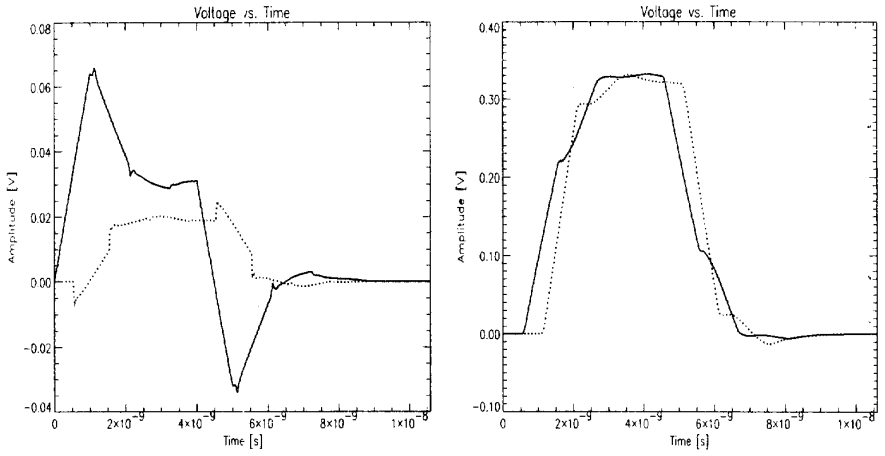

Fig. 11. Voltages at MTL terminals of circuit in Fig. 10. Left: (——) node 3, (· · ·) node 4; Right: (——) node 5; (· · ·) node 6.

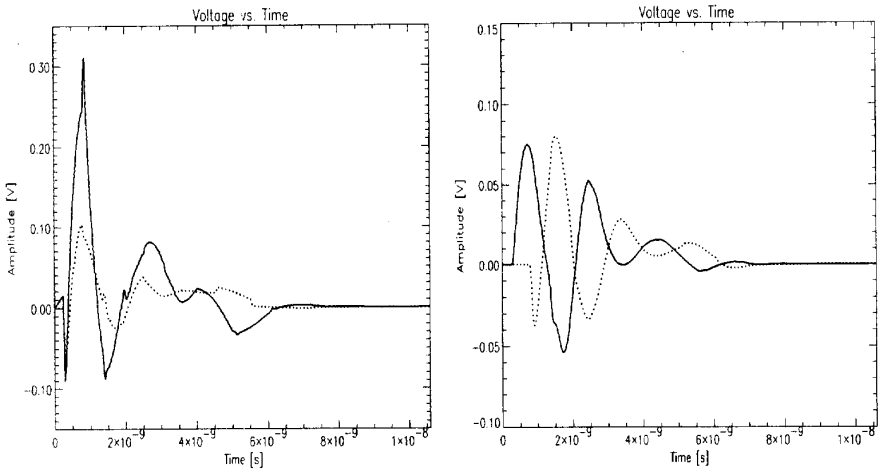

Fig. 12. Voltages at MTL terminals of circuit in Fig. 10 with furniture ESD source applied. Left: (——) node 3, (· · ·) node 4; Right: (——) node 7; (· · ·) node 8.

[m/s]. The time-step is calculated using the Courant condition: $\Delta t = \Delta x/v_p$ [s] where v_p is the largest mode velocity—in this case v_1. The calculated value is $\Delta t = 1.31469 \times 10^{-11}$ [s]. The terminal voltages at nodes 1–4 of Fig. 7 are shown in Fig. 9. The results are in excellent agreement with those of [19].

B. Nonlinear MTL Network Example

For an example of a nonlinear MTL network, we consider an interconnect model with lossy multiconductor transmission lines, shown in Fig. 10. This example is identical to the one solved by Tang *et al.* [20].

The length of both MTL's is 0.1 [m]. The two conductor line has the per-unit-length parameters given by

$$\boldsymbol{L} = \begin{bmatrix} 494.6 & 63.3 \\ 63.3 & 494.6 \end{bmatrix} [\text{nH/m}]$$

$$\boldsymbol{C} = \begin{bmatrix} 62.8 & -4.9 \\ -4.9 & 62.8 \end{bmatrix} [\text{pF/m}]$$

$$\boldsymbol{R} = \begin{bmatrix} 75 & 15 \\ 15 & 75 \end{bmatrix} [\Omega/\text{m}]$$

$$\boldsymbol{G} = \begin{bmatrix} 0.1 & -0.01 \\ -0.01 & 0.1 \end{bmatrix} [\text{S/m}]$$

and the four conductor line has the parameters

$$\boldsymbol{L} = \begin{bmatrix} 494.6 & 63.3 & 7.8 & 0.0 \\ 63.3 & 494.6 & 63.3 & 7.8 \\ 7.8 & 63.3 & 494.6 & 63.3 \\ 0.0 & 7.8 & 63.3 & 494.6 \end{bmatrix} [\text{nH/m}]$$

$$\boldsymbol{C} = \begin{bmatrix} 62.8 & -4.9 & -0.3 & 0.0 \\ -4.9 & 62.8 & -4.9 & -0.3 \\ -0.3 & -4.9 & 62.8 & -4.9 \\ 0.0 & -0.3 & -4.9 & 62.8 \end{bmatrix} [\text{pF/m}]$$

$$\boldsymbol{R} = \begin{bmatrix} 50 & 10 & 1 & 0.0 \\ 10 & 50 & 10 & 1 \\ 1 & 10 & 50 & 10 \\ 0.0 & 1 & 10 & 50 \end{bmatrix} [\Omega/\text{m}]$$

$$\boldsymbol{G} = \begin{bmatrix} 0.1 & -0.01 & -0.001 & 0.0 \\ -0.01 & 0.1 & -0.01 & -0.001 \\ -0.001 & -0.01 & 0.1 & -0.01 \\ 0.0 & -0.001 & -0.01 & 0.1 \end{bmatrix} [\mathrm{S/m}].$$

The nonlinear elements are defined by $V_a = 20i_a + 21.5i^{1/3}a$ and $V_b = 20i_b + 21.5i_b^{1/3}$. The response at various points in the network are shown in Fig. 11, and are in good agreement with the published results in [20]. We also introduce a distributed current source on line one of the first MTL to demonstrate the capability of introducing such sources. We chose a distributed current source waveform representative of a furniture electrostatic discharge, but with smaller amplitude, given by

$$i(t) = 10.0e^{-0.9\cdot 10^9 t} \cdot \sin\left(\frac{\pi t}{1.0\cdot 10^{-9}}\right) [\mathrm{A/m}]. \qquad (21)$$

This source is imposed over the ten finite difference cells in the middle of the conductor (i.e., a 1.0 [cm] segment of line) and some results for the mutual coupling on various lines are shown in Fig. 12. The voltage source $e(t)$ is still active, but the mutual coupling, due to the distributed current source, overwhelms its contribution.

VI. Conclusion

We have described a finite-difference time-domain approach to the solution of MTL network problems having nonlinear junctions. The nonlinear lumped circuit junctions are formulated via the MNA method, and the solution for each time-step of the nonlinear junctions and the MTL's are coupled via a numerical interface, consisting of the last section of each MTL. The use of the FDTD method allows us to incorporate distributed sources on the MTL's to model impinging electromagnetic fields. The finite-difference technique chosen for the MTL's is compatible with that used in Yee type FDTD field solvers, which makes the interfacing with our FDTD field modeler a realistic possibility. We will be investigating the viability of this in the future.

References

[1] C. E. Baum, T. K. Liu, and F. M. Teche, "On the analysis of general multiconductor transmission-line networks," *Interaction Note 350*, Nov. 1978.

[2] J. P. Parmantier, G. Labaume, J. C. Alliot, and P. Degauque, "Electromagnetic topology: junction characterization methods," *Recherche Aerospatiale*, no. 1990-5, pp. 71–82, 1990.

[3] C. E. Baum, "Bounds on norms of scattering matrices," *Electromagn.*, vol. 6, pp. 33–45, 1986.

[4] A. R. Djordjevic, T. K. Sarkar, and R. F. Harrington, "Time-domain response of multiconductor transmission lines," in *Proc. IEEE*, vol. 75, no. 6, pp. 743–764, 1987.

[5] D. Winklestein, M. S. Steer, and R. Pomerleau, "Simulation of arbitrary transmission line networks with nonlinear terminations," *IEEE Trans. Circuits Syst.*, vol. 38, no. 4, pp. 418–422, Apr. 1991.

[6] T. K. Tang and M. S. Nakhla, "Analysis of high-speed VLSI interconnects using the asymptotic waveform evaluation technique," *IEEE Trans. Computer-aided Design Integrated Circuits Syst.*, vol. 11, no. 3, pp. 341–352, Mar. 1992.

[7] A. R. Djordjevic and T. K. Sarkar, "Analysis of time response of lossy multiconductor transmission line networks," *IEEE Trans. Microwave Theory Tech.*, vol. MTT-35, no. 10, pp. 898–907, Oct. 1987.

[8] J. R. Griffith and M. S. Nakhla, "Time-domain analysis of lossy coupled transmission lines," *IEEE Trans. Microwave Theory Tech.*, vol. 38, no. 10, pp. 1480–1487, Oct. 1990.

[9] D. E. Merewether, "A numerical solution for the response of a strip transmission line over a ground plane excited by ionizing radiation," *IEEE Trans. Nucl. Sci.*, vol. 18, no. 8, pp. 398–403, Aug. 1971.

[10] A. K. Agrawal, H. J. Price, and S. H. Gurbaxani, "Transient response of multiconductor transmission lines excited by a nonuniform electromagnetic field," *IEEE Trans. Electromagn. Compat.*, vol. EMC-22, no. 2, pp. 119–129, May 1980.

[11] A. K. Agrawal, H. M. Fowles, L. D. Scott, and S. H. Gurbaxani, "Application of modal analysis to the transient response of multiconductor transmission lines with branches," *IEEE Trans. Electromagn. Compat.*, vol. EMC-21, no. 3, pp. 256–262, Aug. 1979.

[12] W. T. Weeks, "Multiconductor transmission-line theory in the TEM approximation," *IBM J. Res. Develop.*, Nov. 1972, pp. 604–611.

[13] C. R. Paul, *Introduction to Electromagnetic Compatibility*. New York: Wiley, 1992.

[14] ——, "Incorporation of terminal constraints in the FDTD analysis of transmission lines," *IEEE Trans. Electromagn. Compat.*, vol. EMC-36, no. 2, pp. 85–91, May 1994.

[15] J. Vlach and K. Singhal, *Computer Methods for Circuit Analysis and Design*, 2nd ed. New York: Van Nostrand Reinhold, 1994.

[16] C. W. Ho, A. E. Ruehli, and P. A. Brennan, "The modified nodal approach to network analysis," *IEEE Trans. Circuit Syst.*, vol. CAS-22, no. 6, pp. 504–508, June 1975.

[17] J. C. Strikwerda, *Finite Difference Schemes and Partial Differential Equations*. Pacific Grove, CA: Wadsworth & Brooks, 1989.

[18] W. J. McCalla and D. O. Pederson, "Elements of computer-aided circuit analysis," *IEEE Trans. Circuit Theory*, vol. CT-18, no. 1, pp. 14–23, Jan. 1971.

[19] A. R. Djordjevic, T. K. Sarkar, and R. F. Harrington, "Analysis of lossy transmission lines with arbitrary nonlinear terminal networks," *IEEE Trans. Microwave Theory Tech.*, vol. MTT-34, no. 6, pp. 660–665, June 1986.

[20] T. K. Tang, M. S. Nakhla, and J. R. Griffith, "Analysis of lossy multiconductor transmission lines using the asymptotic waveform evaluation technique," *IEEE Trans. Microwave Theory Tech.*, vol. 39, no. 12, pp. 2107–2116, Dec. 1991.

Doru Mardare received the Dipl. Eng. degree in electrical engineering, from the Polytechnic Institute, Bucharest, Romania, in 1982, and the M.E.Sc. degree in electrical engineering, from the University of Western Ontario, London, Canada, in 1994.

From 1982 to 1992, he was a research engineer at the Institute of Computer Technique, in Bucharest. He is currently a research assistant in the Department of Electrical Engineering of the University of Western Ontario, London, Canada. His main areas of interest lie in the time-domain computer modeling of electromagnetic interactions and in computational models of electromagnetic compatibility.

Joe LoVetri (S'84–M'90), photograph and biography not available at the time of publication.